Surface electronic structure of clean and hydrogen-chemisorbed Si_xGe_{1-x} alloy surfaces

Ja-Hum Ku and R. J. Nemanich
Department of Physics, North Carolina State University, Raleigh, North Carolina 27695-8202
(Received 17 June 1996)

The surface electronic states of clean and hydrogen-terminated Si_xGe_{1-x} surfaces were studied with angle-resolved ultraviolet photoelectron spectroscopy (ARUPS). A series of strained and relaxed Si_xGe_{1-x} alloys were grown on Si(100) wafers using electron-beam evaporation in an ultrahigh-vacuum molecular-beam-epitaxy chamber. The growth was followed by *in situ* hydrogen-plasma exposure to obtain H-terminated surfaces. After alloy film growth, a double domain 2×1 reconstruction was observed for the series of clean Si_xGe_{1-x} alloys. A diffuse double domain 2×1 reconstructed surface was obtained after the H-plasma exposure, which implies that the Si(Ge)-H monohydride domains are smaller than the surface terraces. The diffuse peaks were attributed to disorder and incoherence in the H termination rather than a change of the terrace structure. He I (21.21 eV) and Ne I (16.85 eV) resonance lines were employed to identify the surface states or resonances and bulk states of all samples described in this paper. ARUPS spectra of the series of clean and H-terminated Si_xGe_{1-x} alloys were obtained as a function of emission angle along the [010] direction. From measurements of the series of clean Si_xGe_{1-x} alloy surfaces the surface states or resonances due to the dangling bond and the back bond were identified and found to disperse downward from Γ to J'_{ab}. A nondispersive hydrogen-induced surface state or resonance was observed from the series of H-terminated Si_xGe_{1-x} alloy surfaces. The electron affinities of the series of clean and H-terminated Si_xGe_{1-x} alloy surfaces were also measured using ARUPS. The electron affinity of the Si(100) surface was found to be 3.83 eV and those of strained and relaxed Si_xGe_{1-x} (100) surfaces ranged from 3.87 to 4.05 eV. The electron affinity of clean and H-terminated surfaces exhibited the same values. [S0163-1829(96)06244-3]

INTRODUCTION

Several theoretical and experimental studies have been performed to investigate the clean and H-chemisorbed Si(100) and Ge(100) surfaces.[1–9] Johansson, Uhrberg, and Hansson[10] performed angle-resolved ultraviolet photoelectron spectroscopy (ARUPS) experiments on the electronic structure of clean Si(100)2×1 surfaces and hydrogen-chemisorbed Si(100)2×1 surfaces. They observed two hydrogen-induced surface states or resonances (M_1,M_2) on the Si(100)2×1:H surface and a surface state, which is related to the dimer bond, on both the clean and the hydrogen-terminated Si(100)2×1 surfaces. Landemark *et al.*[11] studied the surface electronic structure of Ge(100)2×1 along the [010] direction with ARUPS and a later study[12] explored the [011] direction and the monohydride surface. The studies[11,12] compared the experimentally observed surface structures with calculated surface states and resonances attributed to the dangling-bond state and back-bond resonances. However, to our knowledge, there have been no reports of the surface electronic states of clean and H-terminated Si_xGe_{1-x} surfaces despite the fact that Si_xGe_{1-x} alloys have significant application potential for electronic devices.[13–19]

Silicon and germanium both form in the diamond crystal structure. The materials are completely miscible over the entire compositional range and give rise to alloys also with the diamond crystal structure. Due to the lattice mismatch (4.17%) between silicon and germanium, the epitaxy of Si_xGe_{1-x} on Si results either in a strained (pseudomorphic) layer, if the layers are sufficiently thin, or in an unstrained layer that has been relaxed by the formation of misfit dislocations. Fiory *et al.* suggested that in the case of Si_xGe_{1-x} alloy semiconductors, film thicknesses much greater than the critical thickness may be required before significant relaxation occurs since the onset of relaxation is gradual.[20] Therefore, for heteroepitaxial growth of the Si_xGe_{1-x} alloys, the layers are first pseudomorphically strained and then with increased thickness become partially relaxed and completely relaxed as the film thickness increases far beyond the critical thickness. In general, the band gap of the Si_xGe_{1-x} alloys decreases with increasing Ge content and, due to the presence of strain in the Si_xGe_{1-x} alloys, the strained Si_xGe_{1-x} alloy produces a further reduction in the band gap than the unstrained Si_xGe_{1-x} alloy.[21]

The electronic structure of semiconductor surfaces and interfaces plays a crucial role in the performance of semiconductor devices since the electron transport properties across or along the interfaces within a device structure are directly linked to the electronic structure at the interface. In this study, the electronic structures of clean Si, strained Si_xGe_{1-x} alloy surfaces ($x=0.40$, 0.60, and 0.80) and relaxed Si_xGe_{1-x} alloy surfaces ($x=0$, 0.20, 0.40, and 0.60) were examined using ARUPS with He I and Ne I resonance lines. By comparing the spectra obtained with two different photon energies (21.21 and 16.85 eV), surface states or resonances could be distinguished from bulk states. This is because the measured dispersion of surface states or resonances is, in general, independent of the incident photon energy, while bulk-state energies may change for different excitation energies.[22] A dispersion curve $E_i(k_\parallel)$ was obtained for every sample described here. Surface reconstruction and chemistry were confirmed by *in situ* low-energy electron diffraction (LEED) and Auger electron spectroscopy (AES), respectively. The aim of this set of experiments is to examine the

surface band structures of the clean and H-terminated Si_xGe_{1-x} alloys. Also investigated is the electron affinity of strained and relaxed Si_xGe_{1-x} alloy surfaces as well as clean and H-terminated Si_xGe_{1-x} alloy surfaces.

EXPERIMENTAL PROCEDURES

The Si_xGe_{1-x} thin-film growth, H-plasma exposure, and the surface measurements were all made in ultrahigh vacuum (UHV) without exposure to ambient using an integrated (UHV) system. The system includes molecular-beam epitaxy (MBE), ARUPS, LEED, AES, H-plasma, and loadlock chambers all linked by an UHV transfer line. The system is described in more detail elsewhere.[23,24]

The substrates used in this experiment were 25-mm-diam phosphorous-doped *n*-type Si(100) wafers with a resistivity of 0.8–1.2 Ω cm and a thickness of 0.25–0.30 mm. The wafers were cleaned by exposure to uv ozone for 5 min to remove hydrocarbon contaminants, a HF-based spin etch ($HF:H_2O$:ethanol=1:1:10) to remove the native oxide, and followed by an *in situ* heat cleaning to 850 °C for 10 min in the UHV MBE chamber to eliminate the residual contamination. The wafers were mounted with tantalum wire on a molybdenum sample holder. A 200-Å homoepitaxial silicon buffer layer was deposited on the atomically clean Si(100) substrate to ensure a contamination-free interface. A series of Si_xGe_{1-x} alloys were epitaxially grown on the silicon buffer layers using electron-beam evaporation in the UHV MBE chamber. The base pressure of the MBE chamber was less than 1×10^{-10} Torr. After the initial annealing to clean the surface, the substrate temperature was held at 550 °C during all depositions. The parameters of samples used in this experiment were 300 Å for pure Si and pure Ge and 200, 120, and 40 Å for strained $Si_{0.8}Ge_{0.2}$, $Si_{0.6}Ge_{0.4}$, and $Si_{0.4}Ge_{0.6}$ alloys, respectively. The thicknesses of the strained Si_xGe_{1-x} alloys are less than the critical thickness to ensure a uniformly strained Si_xGe_{1-x} epilayer.[25] To produce relaxed $Si_{0.6}Ge_{0.4}$, $Si_{0.4}Ge_{0.6}$, and $Si_{0.2}Ge_{0.8}$ samples, 8000 Å, 5000 Å, and 3000 Å were deposited, respectively. These thicknesses are far above the respective critical thicknesses.[25] The layer compositions of the deposited Si_xGe_{1-x} alloys were determined by Rutherfold backscattering (RBS) and x-ray absorption fine-structure (XAFS) analysis of similarly prepared Si_xGe_{1-x} alloy films.[26] The maximum difference between calculated composition and composition measured by RBS was found to be 2%, which is within the error of both the XAFS and RBS measurements.[26]

To obtain H-terminated surfaces, the samples were transferred to the remote plasma chamber. The samples were positioned 40 cm downstream relative to the center of the plasma tube, and the H-plasma was generated by exciting the hydrogen gas through a quartz tube with rf radiation (13.56 MHz). The base pressure in the H-plasma chamber was less than 2×10^{-9} Torr. The samples were exposed to the H-plasma under the following conditions: process pressure=15 mTorr; rf power, 20 W; flow rate of H_2 gas, 80 SCCM where SCCM denotes cubic centimeter per minute at STP; and exposure time 1 min. To obtain a 2×1 reconstructed surface the sample temperature was held at 400 °C for pure Si and strained $Si_{0.8}Ge_{0.2}$, while 180 °C was used for the other samples. For higher Ge composition films (Ge content≥40%), the ultraviolet photoelectron spectroscopy (UPS) did not show features due to hydrogen bonding for 400 °C H-plasma exposures. This was also confirmed by previous studies of the surface electronic states of H-terminated Ge(100) surfaces produced by a H-plasma.[27]

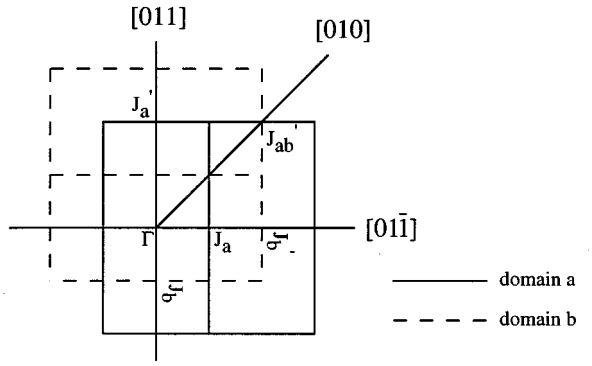

FIG. 1. Surface Brillouin zones of the two-domain Si(100)2×1 surface in the repeated zone scheme.

ARUPS was then employed to investigate the electronic structures of the clean and H-terminated Si_xGe_{1-x} alloy surfaces. The base pressure of the ARUPS chamber was less than 2×10^{-10} Torr with an operating pressure less than 1×10^{-9} Torr. The ARUPS spectra were obtained with a differentially pumped He (Ne) discharge lamp delivering the He I (Ne I) radiation, which has a primary energy of 21.21 eV (16.85 eV). The uv light is incident on the sample at ~45° from the surface normal in the analyzer rotation plane and at ~15° from the surface in the perpendicular plane to the analyzer rotation plane. The photoemitted electrons were analyzed with a 50-mm mean radius hemispherical analyzer (VSW HA 50) with an energy resolution of 0.25 eV and an angular resolution of 2°. The analyzer is mounted on a two-stage goniometer, which allows angle-dependent measurement and can be rotated in the horizontal plane perpendicular to the surface of the sample.

The most frequently observed reconstruction of a clean Si(100) or Ge(100) surface is the double domain 2×1 reconstruction with the two domains at 90° to each other. These two different domains are located on terraces separated by single atomic layer steps.[28] The surface Brillouin zones of the two domains are shown in Fig. 1 for the 2×1 reconstruction. All ARUPS experiments presented here were performed at various emission angles θ_e, along the [010] crystal direction, since along this direction, the surface Brillouin zones of the two domains are equivalent according to the crystal symmetry. All ARUPS spectra of clean surfaces were obtained at emission angles ranging from surface normal to 35° in 5° increments, and the emission angles of the H-terminated samples ranged from surface normal to 40°. Each spectrum was acquired using a 0.005-eV step size and an integration time of ~1 sec at each energy. To improve the signal-to-noise ratio, each sample was scanned five times and the five spectra were summed. After summing, the spectra were subjected to a five-point smoothening to further distinguish the data from the random noise. The peak position was determined with an error of ±0.03 eV. The position of the Fermi level was determined by measuring either a spectrum of a thick metal layer on the semiconductor or a spectrum of

TABLE I. Root-mean-square surface roughness of Si, strained Si_xGe_{1-x} alloys, and relaxed Si_xGe_{1-x} alloys.

Strained	rms roughness (Å)	Relaxed	RMS roughness (Å)
Si (cubic)	2.6±0.5		
$Si_{0.8}Ge_{0.2}$	3.0±0.5		
$Si_{0.6}Ge_{0.4}$	4.9±0.5	$Si_{0.6}Ge_{0.4}$	30.0±1
$Si_{0.4}Ge_{0.6}$	4.5±0.5	$Si_{0.4}Ge_{0.6}$	16.5±1
		$Si_{0.2}Ge_{0.8}$	13.9±1
		Ge	60.2±1

the metallic (Mo) sample holder. Both techniques yielded the same values.

RESULTS

Ex situ atomic force microscopy (AFM) was performed to investigate the surface roughness of the samples. The root-mean-square (rms) surface roughness of the films obtained from AFM experiments are summarized in Table I. The results show that the value of the rms surface roughness of relaxed Si_xGe_{1-x} alloys increased with decreasing Ge content, although the lattice mismatch between Si and Ge decreases as Ge content decreases. We attribute this increase to the increased layer thicknesses used for the relaxed $Si_{0.6}Ge_{0.4}$ alloys as opposed to the thin layers of the relaxed $Si_{0.2}Ge_{0.8}$ alloys. The AFM image of pure Ge showed larger structures on the surface, which resulted in an increased rms surface roughness. This is probably due to the large lattice mismatch between Si and Ge which results in a Stranski-Krastonov growth mode.

The LEED patterns of the clean surfaces exhibited a sharp double domain 2×1 surface reconstruction and those of the H-terminated samples showed a diffuse double domain 2×1 reconstructed surface. The diffuse spots and streaks in the H-terminated surface indicate small domains and/or an incoherence of the dimer domains.[29,30] The AES data obtained prior to and after ARUPS scans indicated Si and Ge peaks with O and C below the detection limit.

The ARUPS spectra of the clean and H-terminated Si(100) and Ge(100) surfaces were obtained with two different photon energies (21.21 and 16.85 eV) and compared to the data reported previously.[10,11,31] The ARUPS spectra of the clean Si(100) surface, recorded with He I and Ne I excitations, for various emission angles along the [010] direction are shown in Fig. 2.

Several structures that have been attributed to emission from occupied surface states were observed for a clean Si(100)2×1 surface. The surface state *A* (following the notation of Johansson *et al.*[31]) observed at 0.88 eV below E_F at Γ disperses downward to 1.58 eV below E_F at J'_{ab}. Surface state *B* was detected at 1.00 eV below E_F from an emission angle of ~25° for spectra with He I (21.21 eV) photon energy. The state *G* observed at 30° and 35° emission angles from the clean surface with He I excitation shows the same behavior as the state that had previously been related to a dimer bond surface state.[31] More recent studies have indicated that the feature is a bulk state.[10] The surface state *D*, which has been associated with the back bond, was also identified on the Si(100)2×1 surface. From the spectra of the

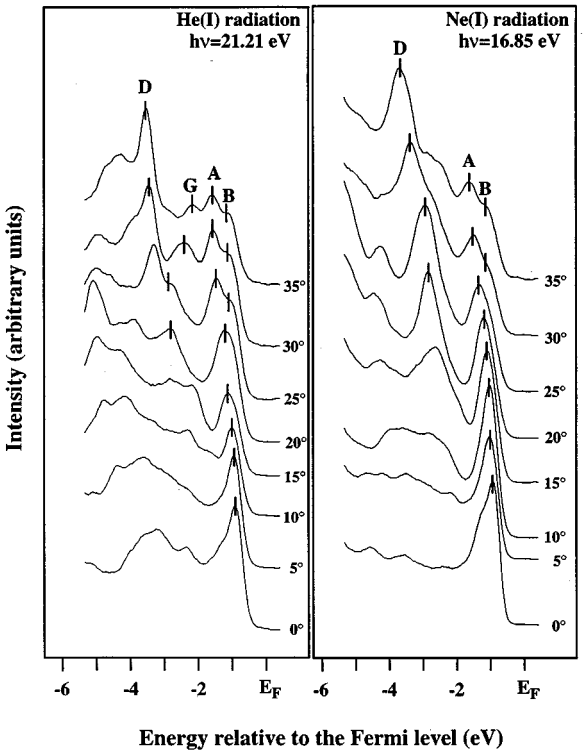

FIG. 2. ARUPS spectra of a clean Si(100)2×1 surface recorded as a function of emission angle θ_e in the [010] azimuthal direction, obtained with (a) He I (21.21 eV) excitation and (b) Ne I (16.85 eV) excitation. The peaks labeled *A* and *B* indicate the surface states associated with dangling-bond states; peaks *G* and *D* indicate the surface states related to the dimer bond states and the back bond states, respectively.

clean Ge(100)2×1 surface, a surface state associated with the dangling bond was found at 0.86 eV below E_F at Γ and the state exhibited a downward dispersion towards J'_{ab}. A surface state that may be related to the back bond was also observed at −3.09 eV relative to E_F around the J'_{ab} point for the clean Ge(100)2×1 surface. However, similar to the results reported by Landemark *et al.*,[11] there was no evidence of the calculated dimer bond surface state or resonance at ~2.2 eV below E_F at J'_{ab}.

After H exposure of the Si(100)2×1 surface, two H-induced surface states or resonances M_1 and M_2 (following the notation of Johansson, Uhrberg, and Hansson[10]) were observed at −4.95 and −5.95 eV relative to the Fermi level, respectively, for an emission angle of 35°. In the spectra of the monohydride Ge(100) surface, one H-induced surface state or resonance was identified at 5.30 eV below E_F at an emission angle of 35°. These results showed close agreement with previously reported data, although the absolute positions differ slightly.[10,11,31]

Figures 3(a) and 3(b) show ARUPS spectra of the clean strained $Si_{0.8}Ge_{0.2}$ surface, recorded as a function of emission angle θ_e with 21.21 and 16.85 eV photon energies, respectively. Two surface states, marked *A* and *D* in Figs. 3(a) and 3(b), were observed from the spectra of the clean surface. The state *A* disperses from 0.93 eV below E_F at Γ down to 1.40 eV below E_F at J'_{ab}. The surface state *D*, which begins to develop at an emission angle of 20°, shows a downward

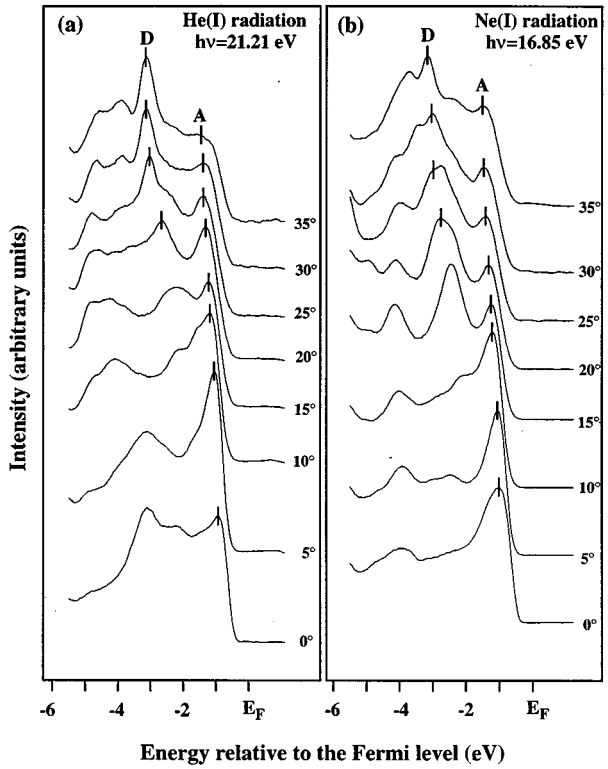

FIG. 3. ARUPS spectra of a clean strained $Si_{0.8}Ge_{0.2}$ alloy surface recorded as a function of emission angle θ_e in the [010] azimuthal direction, obtained with (a) He I (21.21 eV) excitation and (b) Ne I (16.85 eV) excitation. The peaks labeled *A* and *D* indicate the surface states related to dangling-bond states and back-bond states, respectively.

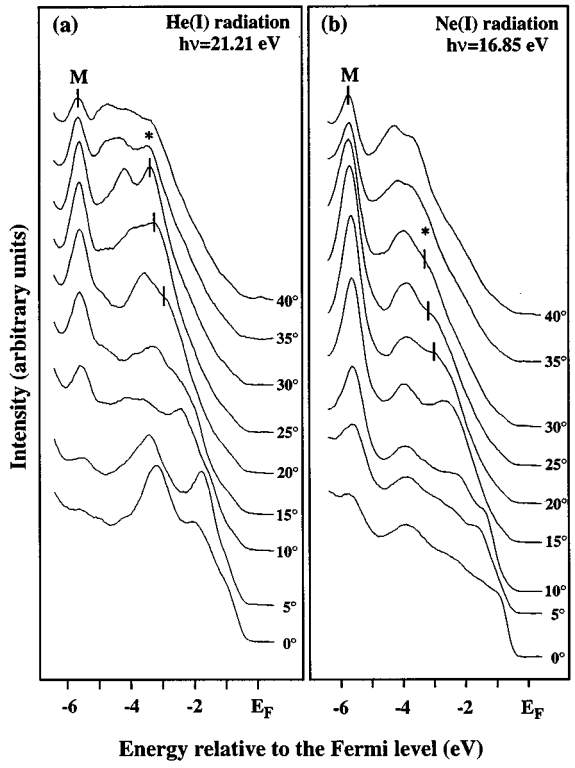

FIG. 4. ARUPS spectra of monohydride strained $Si_{0.8}Ge_{0.2}$ alloy surface recorded as a function of emission angle θ_e in the [010] azimuthal direction obtained with (a) He I (21.21 eV) excitation and (b) Ne I (16.85 eV) excitation. The peak labeled *M* indicates the hydrogen-induced surface state and the asterisk indicates a state with an energy near *D* of the clean surface.

dispersion to J'_{ab} of 1.01 eV. The corresponding spectra from the monohydride surface are shown in Figs. 4(a) and 4(b). An H-induced surface state or resonance, labeled *M* in Figs. 4(a) and 4(b), was observed at ~5.60 eV below E_F on the monohydride surface. The surface state *D* was largely absent on the monohydride surface. There is, however, an identifiable weak feature (marked by an asterisk) that occurs at the same energy as state *D* in the corresponding spectra from the clean surface.

ARUPS spectra of the clean relaxed $Si_{0.2}Ge_{0.8}$ surface and the H-terminated relaxed $Si_{0.2}Ge_{0.8}$ surface, recorded as a function of emission angle θ_e, with 21.21 and 16.85 eV photon energies, are shown in Figs. 5 and 6, respectively. The surface state *A* observed at -0.80 eV relative to E_F at Γ disperses downward to -1.52 eV relative to E_F at J'_{ab}. The surface state *D* was also identified in the spectra of the clean surface. A H-induced surface state or resonance was observed at 5.26 eV below E_F at an emission angle of 0° after H-plasma exposure of the $Si_{0.2}Ge_{0.8}$ surface. This state *M* disperses downward initially and then remains at 5.44 eV below E_F, which is a higher energy than the position of the *M* state on the monohydride strained $Si_{0.8}Ge_{0.2}$ surface. Here also the state *D* is largely absent in the monohydride surface, but a weak feature occurs at a similar energy as *D* in the corresponding clean spectra. These surface states *A*, *D*, and *M* are noted in Figs. 5 and 6.

The ARUPS system was also employed to measure the electron affinities of the series of clean and H-terminated $Si_xGe_{1-x}(100)2\times1$ surfaces. The electron affinity of the semiconductor can be related to the photoemission spectra through the relation

$$\chi = h\nu - W - E_g,$$

where $h\nu$ is the incident energy (21.21 eV for He I radiation), E_g is the band gap of the semiconductor, and *W* is the width of the ARUPS spectrum. To obtain the width of the spectrum it is usually necessary to bias the sample such that low-energy electrons can overcome the work function of the analyzer. The width of the spectrum was obtained by measuring the energy difference between the onset of the spectrum (valence-band maximum) and the cutoff of the spectrum by the vacuum level (low-energy limit). The measured electron affinities are summarized in Table II and plotted in Fig. 7. The band gap of the Si_xGe_{1-x} alloys[21] is also shown in the figure. Using the electron affinity data and the reported band gap, the relative energies of the conduction band and the valence band of the strained and the unstrained Si_xGe_{1-x} alloys are plotted with respect to the vacuum level. The conduction band and the valence band of the strained Si_xGe_{1-x} alloys are marked as solid lines and those of the unstrained Si_xGe_{1-x} alloys are marked as dashed lines.

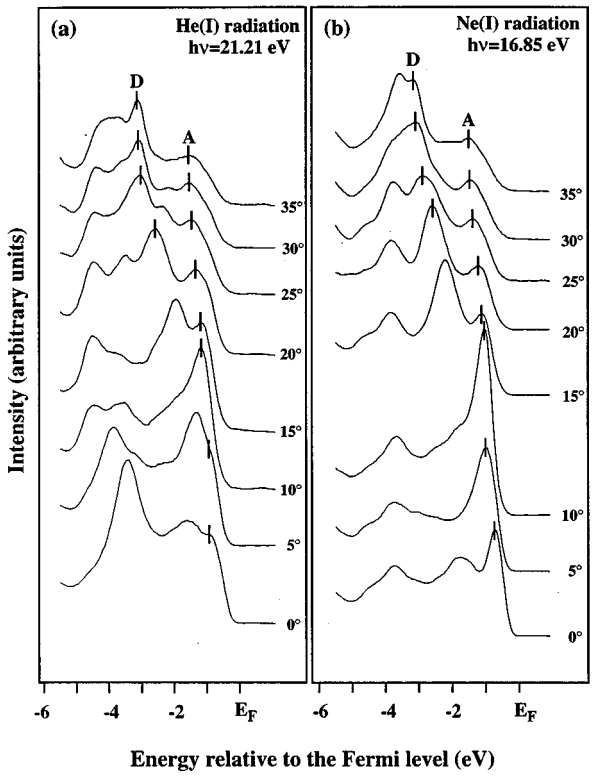

FIG. 5. ARUPS spectra of a clean relaxed $Si_{0.2}Ge_{0.8}$ alloy surface recorded as a function of emission angle θ_e in the [010] azimuthal direction, obtained with (a) He I (21.21 eV) excitation and (b) Ne I (16.85 eV) excitation. The peaks labeled *A* and *D* indicate the surface states related to dangling-bond states and back-bond states, respectively.

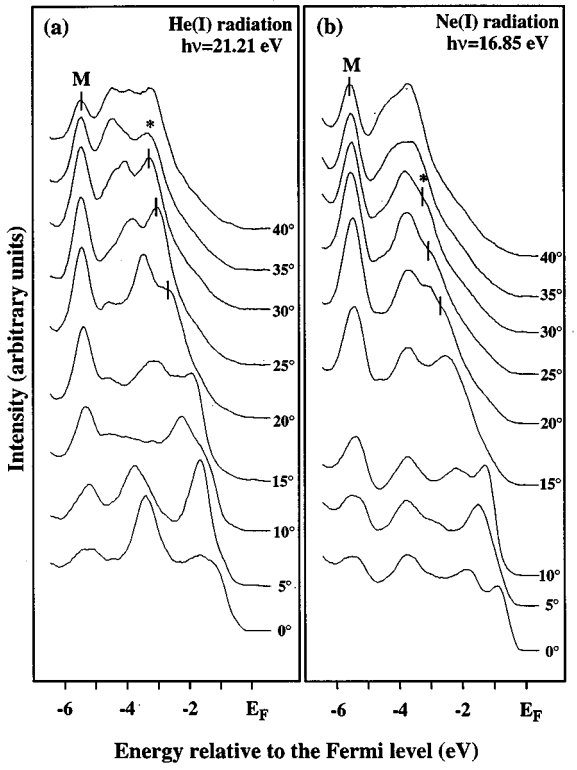

FIG. 6. ARUPS spectra of monohydride relaxed $Si_{0.2}Ge_{0.8}$ alloy surface recorded as a function of emission angle θ_e in the [010] azimuthal direction, obtained with (a) He I (21.21 eV) excitation and (b) Ne I (16.85 eV) excitation. The peak labeled *M* indicates the hydrogen induced surface state and the asterisk indicates a state with an energy near *D* of the clean surface.

DISCUSSION

Consider first the identification of the states on the clean surfaces. In Figs. 3(a) and 3(b), two surface states *A* and *D* are identified by comparing the clean surface spectra obtained with He I and Ne I photon energies. The origin of the features can be determined by comparing the spectra from the monohydride and the clean surfaces shown in Figs. 3 and 4. In Figs. 4(a) and 4(b), it can be noted that the surface state *A* was completely removed by hydrogen chemisorption. This indicates that the *A* state is a surface state most likely attributed to the dangling-bond state. The surface state, denoted *D*, which appears at emission angles $\geqslant 20°$ and disperses downwards towards J'_{ab}, was also observed for the clean surface. A weak feature was observed in the corresponding spectra of the monohydride surface. This will be discussed further below. A strong H-induced surface state or resonance observed on the monohydride surface shows a nondispersive character. This indicates that this state (*M*) is strongly localized in the [010] direction.

To explain the structure *D*, the experimental results shown in Figs. 3 and 4 may be compared to the earlier theoretical and experimental band structures of Si(100) and Ge(100) surfaces. Uhrberg *et al.*[32] and Koke, Goldmann, and Mönch[33] conducted ARUPS experiments on Si(100) surfaces. They observed the *D* state, which disperses downward, and suggested that this state was associated with the dimer bond. Recently, Johansson *et al.*[31] studied the electronic structure of the Si(100)2×1 surface with polarization-dependent angle-resolved photoemission and obtained surface band dispersions of single-domain 2×1 surfaces along the [011] and [011] directions. They also compared the electronic structure of the single-domain Si(100)2×1 surface with the electronic structure of the two-domain surface re-

TABLE II. Measured electron affinities of the 2×1 reconstructed (100) surfaces of Si, strained Si_xGe_{1-x} alloys, and relaxed Si_xGe_{1-x} alloys. The value for Si is shown in the strained and the relaxed columns for comparison.

$Si_xGe_{1-x}(100)$ surface	Electron affinity χ of the clean surface (eV)	Electron affinity χ of the H-terminated surface (eV)
	Strained	
Si (cubic)	3.82±0.03	3.83±0.03
$Si_{0.8}Ge_{0.2}$	3.91±0.03	3.90±0.03
$Si_{0.6}Ge_{0.4}$	3.93±0.03	3.93±0.03
$Si_{0.4}Ge_{0.6}$	3.96±0.03	3.96±0.03
	Relaxed	
Si (cubic)	3.82±0.03	3.83±0.03
$Si_{0.6}Ge_{0.4}$	3.88±0.03	3.87±0.03
$Si_{0.4}Ge_{0.6}$	3.88±0.03	3.88±0.03
$Si_{0.2}Ge_{0.8}$	3.91±0.03	3.90±0.03
Ge	4.04±0.03	4.05±0.03

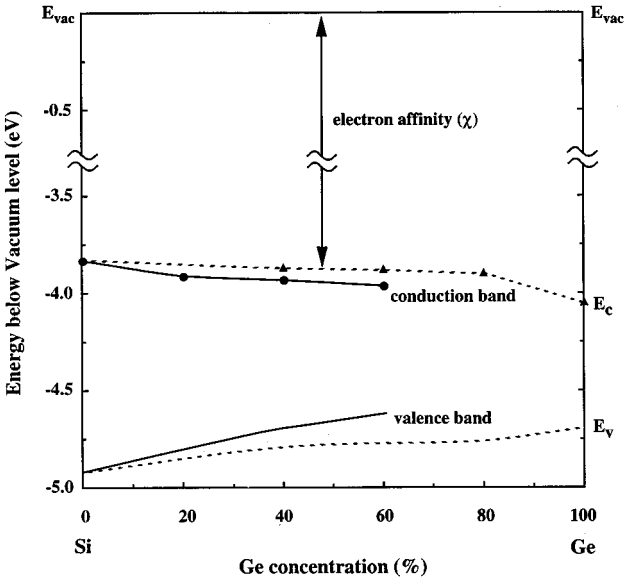

FIG. 7. Valence- and conduction-band edges of the 2×1 reconstructed (100) surfaces of Si, strained Si_xGe_{1-x} alloys, and unstrained Si_xGe_{1-x} alloys. The conduction band and the valence band of the strained Si_xGe_{1-x} alloys are marked with solid lines and those of the unstrained Si_xGe_{1-x} alloys are marked with dashed lines. Circles and triangles indicate the measured electron affinities of the strained and relaxed $Si_xGe_{1-x}(100)2\times1$ surfaces, respectively. The band gap data reported by People (Ref. 18) were used to position the valence band.

corded in the [010] direction, as well as with the theoretical band-structure calculation of Pollmann *et al.*[34,35] which was based on an asymmetric dimer model. They identified the surface states that may be related to the back bond and the dimer bond. Contrary to the assignments in Refs. 32 and 33, it was suggested that the *D* state, which disperses downward towards J'_{ab}, was related to the back-bond state. Landermark *et al.*[11,12] also observed this *D* state from the Ge(001)2×1 surface and noted that the surface structure of this state coincided with the calculated surface structure of the back bond. By comparing these results with the data of the $Si_{0.8}Ge_{0.2}$ surface, the *D* state in Figs. 3 and 4 may be related to the back-bond state rather than the dimer-bond state.

In the study of Koke, Goldmann, and Mönch the structure *D* was observed on clean and monohydride Si(100) surfaces but not on the dihydride surface.[33] In contrast, it was reported that the structure *D* was not observed on monohydride surface[31] and thus is sensitive to chemisorption on the surface.[31,32] Furthermore, it was shown by Landemark *et al.* that a state was observed from monohydride Ge(001)2×1 that showed dispersion similar to state *D* from the clean surface.[12] The measurements and analysis indicated that this state was, in fact, a bulk state. In our studies we observed a weak feature that apparently corresponded to state *D* on two-domain H-terminated 2×1 Si_xGe_{1-x} alloy surfaces. It is, however, likely that this feature is actually a bulk state with the same origin as noted in Ref. 12.

In photoemission experiments on well-ordered surfaces, $k_\parallel$ of a large fraction of the emitted electrons is conserved within a surface reciprocal lattice wave vector G_s.[36] The relations for the parallel wave vectors are given by

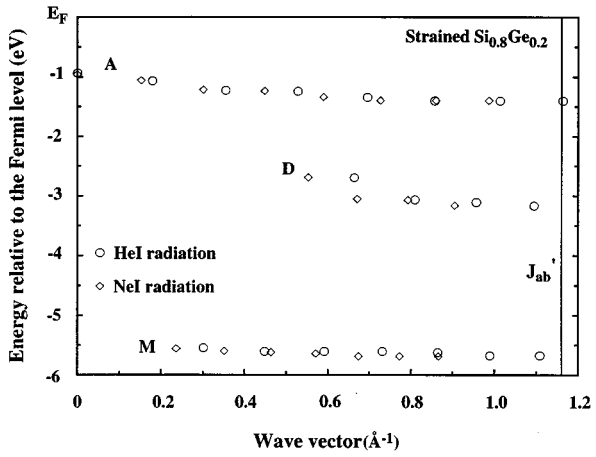

FIG. 8. Surface band structure of the 2×1 reconstructed strained $Si_{0.8}Ge_{0.2}(100)$ surface in the [010] azimuthal direction, recorded with 21.21 eV photon energy (○) and 16.85 eV photon energy (◇). The surface states associated with the dangling bond, back bond, and H-induced surface states are labeled *A*, *D*, and *M*, respectively.

$$\mathbf{k}_\parallel = \mathbf{k}_{f\parallel} + \mathbf{G}_s \approx \mathbf{k}_{i\parallel} + \mathbf{G}_s ,$$

$$k_\parallel = |\mathbf{k}_\parallel| = \frac{\sqrt{2mE_{\rm kin}}}{\hbar} \sin\theta_e ,$$

where $\mathbf{k}_{i\parallel}$ and $\mathbf{k}_{f\parallel}$ are the wave vectors of the initial and final states of the photoelectrons, respectively. By measuring the kinetic energy $E_{\rm kin}$ of electrons as a function of emission angle θ_e, a dispersion curve $E_i(k_\parallel)$ can be obtained.

The band dispersions of the surface states or resonances for the peaks of *A*, *D*, and *M* of strained $Si_{0.8}Ge_{0.2}$ (Figs. 3 and 4) are summarized in Fig. 8. The surface band structure of the 2×1 reconstructed relaxed $Si_{0.2}Ge_{0.8}(100)$ surface is also shown in Fig. 9. The surface states previously associated

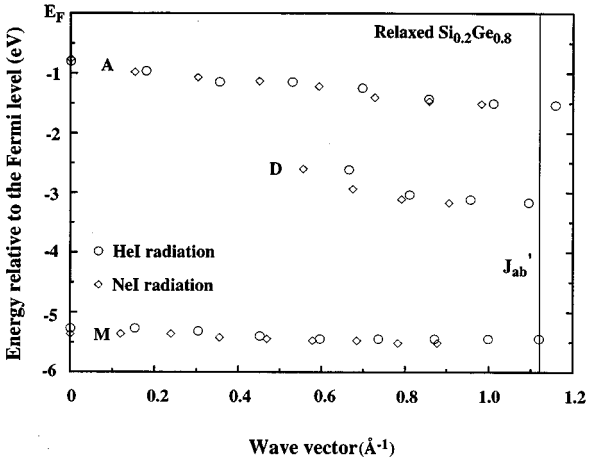

FIG. 9. Surface band structure of the 2×1 reconstructed relaxed $Si_{0.2}Ge_{0.8}(100)$ surface in the [010] azimuthal direction, recorded with 21.21 eV photon energy (○) and 16.85 eV photon energy (◇). The surface states associated with the dangling bond, back bond, and H-induced surface states are labeled *A*, *D*, and *M*, respectively.

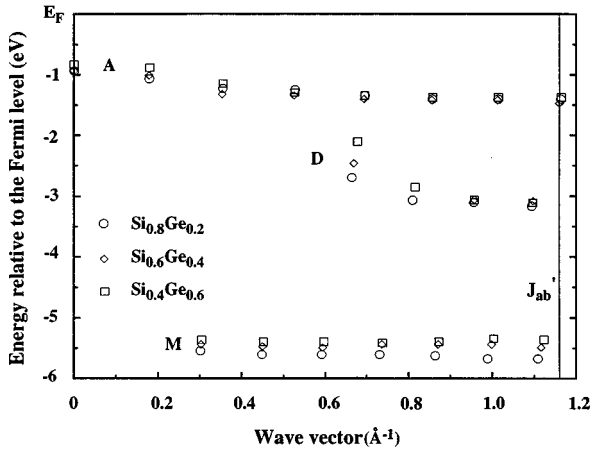

FIG. 10. Surface band structure of the 2×1 reconstructed strained $Si_xGe_{1-x}(100)$ surfaces in the [010] azimuthal direction, recorded with 21.21 eV photon energy. The surface states associated with the dangling bond, back bond, and H-induced surface states are marked as *A*, *D*, and *M*, respectively.

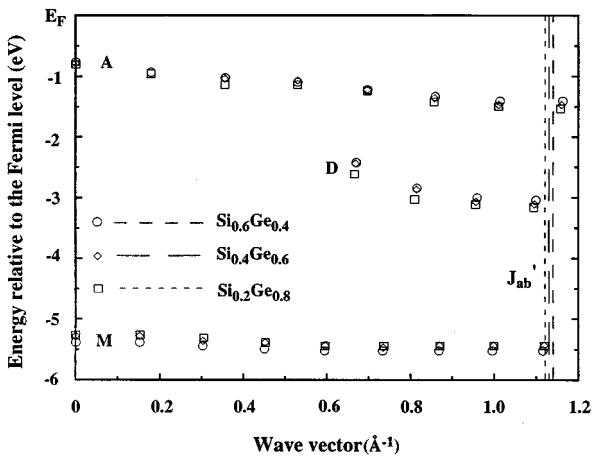

FIG. 11. Surface band structure of the 2×1 reconstructed relaxed $Si_xGe_{1-x}(100)$ surfaces in the [010] azimuthal direction, recorded with 21.21 eV photon energy. The surface states associated with the dangling bond, back bond, and H-induced surface states are marked as *A*, *D*, and *M*, respectively.

with the dangling bond, back bond, and H-induced surface states or resonances are marked as *A*, *D*, and *M*, respectively.

In general, the positions of the surface states from the spectra with He I photon energy are in good agreement with those from the spectra with Ne I photon energy. However, Figs. 8 and 9 show that the band structure at $k_{\|}=\sim 0.6$ Å^{-1} of state *D* excited with He I radiation exhibits a small energy difference from the *D* state obtained with Ne I excitation. For pure Si and pure Ge, the structure related to the back-bond state has a surface resonance character due to the overlap with the projected bulk band structure.[11,31] Furthermore, it was reported that the positions of state *D* and the bulk states are quite close at $k_{\|}=\sim 0.6$ Å^{-1}.[33] Therefore, it can be suggested that the state *D* at $k_{\|}=\sim 0.6$ Å^{-1} is mixed with a bulk state and shows a dependence on the incident photon energy due to partial bulk character.

The band dispersions for the surface states or resonances *A*, *D*, and *M* of 2×1 reconstructed strained and relaxed $Si_xGe_{1-x}(100)$ surfaces along the [010] azimuthal direction, recorded with 21.21 eV photon energy, are plotted in Figs. 10 and 11, respectively. To obtain the value of J'_{ab} of the relaxed Si_xGe_{1-x} alloys, it is necessary to calculate the lattice constant $a_{\|}$ of each sample. When calculating the parallel lattice constant of the relaxed Si_xGe_{1-x} alloys, it was assumed that Vegard's law holds for the Si_xGe_{1-x} alloys and that the films were totally relaxed.

Figure 12 summarizes the average energy of the H-induced surface state band (*M*) of the strained and relaxed Si_xGe_{1-x} alloys. With increasing Ge content the band appears at lower energy relative to the valence-band maximum. This can be understood since the position of the H-induced peak (M_2) of Si (5.95 eV below E_F at an emission angle 30°) is observed at a larger relative energy than that of Ge (5.31 eV below E_F at an emission angle 30°). We also find that the relative position of the H-induced peak for the strained Si_xGe_{1-x} alloys with $x=0.4$ and 0.6 is slightly decreased from that of the unstrained alloys. We note that the strained alloys will exhibit a smaller band gap than the unstrained alloys (for the same concentration). Thus it appears that the position of the H-induced peak relative to the valence-band maximum decreases as the band gap decreases, and this trend is observed both as Ge concentration increases and for the strained vs unstrained alloys.

The electron affinity is an important surface parameter for characterizing interfaces of semiconductors. The electron affinity is sensitive to the surface dipole, which is the result of any modification in the surface electron charge distribution. This can be, for example, by adsorption of atoms or molecules on a clean surface. The electron affinity can be obtained by subtracting from the work function (ϕ) the difference in energy between the Fermi level and the conduction band minimum ($\chi=\phi-[E_c-E_F]$). The results presented here indicate that the electron affinity of the strained $Si_xGe_{1-x}(100)$ surface is only slightly larger than that of the relaxed $Si_xGe_{1-x}(100)$ surface of the same Ge content, although the strained and the unstrained Si_xGe_{1-x} alloys ex-

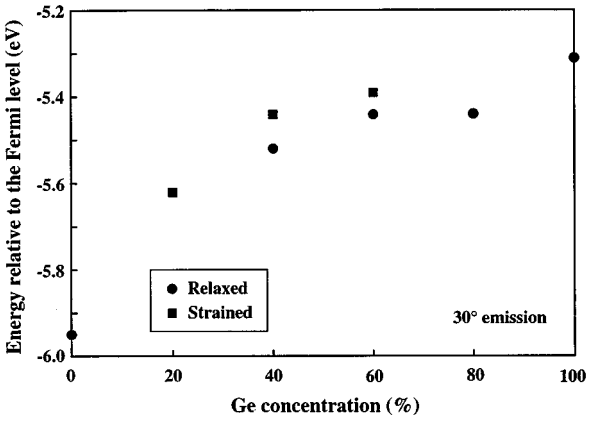

FIG. 12. Energy of the H-induced surface state band versus alloy concentration. While the bands are relatively flat, the data shown here were all obtained from spectra at an emission angle of 30°.

hibit substantial differences in the band gap for identical alloy concentrations. This implies that most of the energy difference in the band gap of a series of Si_xGe_{1-x} alloys is present in the valence-band edge.

In a study of H adsorption on Ge(100), a work function change $\Delta\phi$ was observed after H exposure.[37] The experimental results showed that after the initial steep $\Delta\phi$ increases for low coverage of hydrogen, the $\Delta\phi$ saturated at a value less than $+0.05$ eV in going from Ge(100)2×1 to Ge(100)2×1:H. This suggests that the work function was not affected by H-passivation. Fujiwara also reported a decrease in the work function ($\sim$0.4 eV) upon hydrogenation on Si(100) surface.[38] However, it can be noted that the UPS spectra of the H-terminated Si surface in Ref. 38 shows a broad peak at $\sim$8 eV below the Fermi level, which may be attributed to the non-bonding p orbitals of O present on the surface.[39] This indicates that the H-terminated Si surface, which was used in the study of Fujiwara, was contaminated with oxygen. In the results reported here, the measured electron affinity of the $Si_xGe_{1-x}(100)$ surface is essentially identical for clean and H-terminated Si_xGe_{1-x} surfaces of the same sample. This is essentially consistent with the results reported by Surnev and Tikhov.[37]

CONCLUSIONS

The surface state band structures of a series of clean and H-terminated Si_xGe_{1-x} alloy surfaces were obtained using ARUPS. The surface state due to the dangling bond was identified from the series of clean strained and relaxed Si_xGe_{1-x} alloy surfaces. The ARUPS spectra of H-terminated Si_xGe_{1-x} alloy surfaces exhibited a hydrogen-induced surface state corresponding to the Si(Ge)-H bond. Another surface state, which was related to the back bond, was observed from the clean Si_xGe_{1-x} alloy surfaces.

The electron affinities of the series of clean and H-terminated $Si_xGe_{1-x}(100)2\times1$ surfaces were measured and ranged from 3.83 to 4.05 eV. The results show that the electron affinity of the strained $Si_xGe_{1-x}(100)$ surface is larger than that of the relaxed $Si_xGe_{1-x}(100)$ surface with the same Ge content, while the electron affinity was unchanged by hydrogen passivation for the same sample.

ACKNOWLEDGMENTS

The authors thank Z. Wang, J. Barnak, H. Ying, R. Carter, and S. King for their invaluable help. This work is supported in part by the NSF under Grant No. DMR9633547.

[1] F. J. Himpsel and F. E. Eastman, J. Vac. Sci. Technol. **16**, 767 (1979).
[2] A. L. Wachs, T. Miller, T. C. Hsieh, A. P. Shapiro, and T. C. Chiang, Phys. Rev. B **32**, 2326 (1985).
[3] J. A. Appelbaum, G. A. Baraff, D. R. Hamann, H. D. Hagstrum, and T. Sakurai, Surf. Sci. **70**, 654 (1978).
[4] J. A. Appelbaum, G. A. Baraff, and D. R. Hamann, Phys. Rev. B **14**, 588 (1976).
[5] J. E. Rowe and H. Ibach, Phys. Rev. Lett. **32**, 421 (1974).
[6] L. Papagno, X. Y. Shen, J. Anderson, G. S. Spagnolo, and G. J. Lapeyre, Phys. Rev. B **34**, 7188 (1986).
[7] Y. L. Chabal, Surf. Sci. **168**, 594 (1986).
[8] J. J. Boland, Phys. Rev. Lett. **65**, 3325 (1990).
[9] S. Ciraci, R. Butz, E. M. Oellig, and H. Wagner, Phys. Rev. B **30**, 711 (1984).
[10] L. S. O. Johansson, R. I. G. Uhrberg, and G. V. Hansson, Surf. Sci. **189/190**, 479 (1987).
[11] E. Landemark, R. I. G. Uhrberg, P. Krüger, and J. Pollmann, Surf. Sci. **236**, L359 (1990).
[12] E. Landemark, C. J. Karlsson, L. S. O. Johansson, and R. I. G. Uhrberg, Phys. Rev. B **49**, 16 523 (1994).
[13] J. N. Burghartz, J. H. Comfort, G. L. Patton, B. S. Meyerson, J. Y.-C. Sun, J. M. C. Stork, S. R. Mader, C. L. Stanes, G. J. Scilla, and B. J. Ginsberg, IEEE Electron Device Lett. **11**, 288 (1990).
[14] G. L. Patton, J. H. Comfort, B. S. Meyerson, E. F. Crabbé, G. J. Scilla, E. D. Frésart, J. M. C. Stork, J. Y.-C. Sun, D. L. Harame, and J. N. Burghartz, IEEE Electron Device Lett. **11**, 171 (1990).
[15] J. C. Sturm, E. J. Prinz, and C. W. Magee, IEEE Electron Device Lett. **12**, 303 (1991).
[16] R. D. Thompson, K. N. Tu, J. Angillelo, S. Delage, and S. S. Iyer, J. Electrochem. Soc. **135**, 3161 (1988).
[17] T. L. Lin, T. George, E. W. Jones, A. Ksendozov, and M. L. Huberman, Appl. Phys. Lett. **60**, 380 (1988).
[18] R. People, IEEE J. Quantum Electron. **QE-22**, 1696 (1986).
[19] *Silicon Molecular Beam Epitaxy*, edited by E. Kasper and J. C. Bean (CRC, Boca Raton, FL, 1988).
[20] A. T. Fiory, J. C. Bean, R. Hull, and S. Nakahara, Phys. Rev. B **31**, 4063 (1985).
[21] R. People, Phys. Rev. B **32**, 1405 (1985).
[22] G. V. Hansson and R. I. G. Uhrberg, Surf. Sci. Rep. **9**, 197 (1988).
[23] J. van der Weide and R. J. Nemanich, J. Vac. Sci. Technol. B **10**, 1940 (1992).
[24] J. van der Weide and R. J. Nemanich, Phys. Rev. B **49**, 13 629 (1994).
[25] R. People and J. C. Bean, Appl. Phys. Lett. **47**, 322 (1985).
[26] D. B. Aldrich, R. J. Nemanich, and D. E. Sayers, Phys. Rev. B **50**, 15 026 (1994).
[27] J. Cho and R. J. Nemanich, Phys. Rev. B **46**, 12 421 (1992).
[28] J. E. Griffith, G. P. Kochanski, J. A. Kubby, and P. E. Wierenga, J. Vac. Sci. Technol. A **7**, 1914 (1989).
[29] G. Ertl and J. Kuppers, *Low Energy Electron and Surface Chemistry* (VCH, Weinheim, 1985).
[30] J. Ihm, D. H. Lee, J. D. Joannopoulos, and A. N. Berker, J. Vac. Sci. Technol. B **1**, 705 (1983).
[31] L. S. O. Johansson, R. I. G. Uhrberg, P. Mårtensson, and G. V. Hansson, Phys. Rev. B **42**, 1305 (1990).
[32] R. I. G. Uhrberg, G. V. Hansson, J. M. Nicholls, and S. A. Flodström, Phys. Rev. B **24**, 4684 (1981).
[33] P. Koke, A. Goldmann, and W. Mönch, Surf. Sci. **152/153**, 1001 (1985).
[34] J. Pollmann, R. Kalla, P. Krüger, A. Mazur, and G. Wolfgarten, Appl. Phys. A **41**, 21 (1986).
[35] J. Pollmann, P. Krüger, and A. Mazur, J. Vac. Sci. Technol. B **5**, 945 (1987).
[36] A. Zangwill, *Physics at Surfaces* (Cambridge University Press,

Cambridge, 1988), pp. 75–76.
[37] L. Surnev and M. Tikhov, Surf. Sci. 138, 40 (1984).
[38] K. Fujiwara, Phys. Rev. B **26**, 2036 (1982).
[39] T. P. Schneider, J. Cho, Y. L. Chen, D. M. Maher, and R. J. Nemanich, in *Surface Chemical Cleaning and Passivation for Semiconductor Processing*, edited by G. S. Higashi, E. A. Irene, and T. Ohmi, MRS Symposia Proceedings No. 315 (Materials Research Society, Pittsburgh, 1993), p. 197.